Electronic Supporting Information

Plasma-treated Ti^{3+}-doped sodium titanate nanosheet arrays on titanium foil as a lithiophilic current collector for stable lithium metal

Qi Zhang, Jingyi Luan, Dan Sun, Yougen Tang, and Haiyan Wang*

Hunan Provincial Key Laboratory of Chemical Power Sources,Hunan Provincial Key Laboratory of Efficient and Clean Utilization of Manganese Resources, College of Chemistry and Chemical Engineering, Central South University, Changsha 410083, China, E-mail: wanghy419@csu.edu.cn

Experimental section

2.1. Synthesis of Ti^{3+} doped sodium titanate nanosheet arrays on titanium foil

Titanium foil (3×3×0.03 cm) was first cleaned by sequential ultrasonic treatment in acetone and ethanol, then rinsed with deionized water to remove the impurity on the surface. The cleaned titanium foil was transferred into a Teflon-lined autoclave with 50 ml of 1 M NaOH solution. The autoclave was sealed and maintained at 180 ºC for 24 h. After cooling down to room temperature, the foil was washed by deionized water and dried at 80 ºC. The product was denoted as TF@NTO. The as-prepared TF@NTO was then treated by Ar/H_2 plasma (13.56 MHz radio frequency source) with the power of 200 W and the pressure of 10 Pa for 2 h, which was denoted as TF@P-NTO.

2.2. Characterizations

X-ray diffraction (XRD) patterns were recorded on a Bruker D8 X-ray diffractometer with Cu Kα radiation ($\lambda = 1.5406$ Å). Raman spectra were obtained using a LabRAM Aramis (HORIBA Jobin Yvon) spectrometer from 200 to 1000 cm^{-1}. X-ray photoelectron spectroscopy (XPS) was performed by utilizing a K-Alpha1063 spectrometer. Scanning electron microscopy (SEM, Nova NanoSEM 230) was used to observe the morphologies of the products.

2.3. Electrochemical measurements

The electrochemical lithium plating/stripping measurements were conducted in 2016 type coin cells with the as-prepared current collectors (round disk of 1.2 cm in diameter) as the work electrodes and lithium foils as the counter electrodes. The electrolyte was 1 M bis (trifluoromethane) sulfonamide lithium salt (LITFSI) in 1:1 (v/v) 1, 3-dioxolane (DOL) and 1, 2-dimethoxyethane (DME) with 1 wt% $LiNO_3$. The separator was Celgard membranes K2045 dried at 50 °C for 2 h before use. A Neware CT-3008W battery testing system was employed for the galvanostatic charge/discharge tests. The cells were first activated between 0.01 and 1 V at 0.05 mA cm^{-2} for three cycles. The Coulombic efficiency tests were performed using the galvanostatic discharge process with a specific capacity of 1 mAh cm^{-2} at 1 mA cm^{-2} for the lithium plating and the galvanostatic charge process with a cut-off potential of 1 V (vs. Li^+/Li) at

1 mA cm^{-2} for the lithium stripping. Electrochemical impedance spectroscopy (EIS) was conducted on a CHI660D electrochemical workstation with a frequency range from 10^5 to 10^{-2} Hz. For the symmetric test, 4 mAh cm^{-2} of lithium was first plated on the current collector at 1 mA cm^{-2}. Then the obtained lithium anodes were extracted from the cell and two identical anodes were reassembled into symmetric batteries. Full cells were assembled to evaluate the feasibility of the as-prepared lithium anodes paired with sulfur/acetylene black (S/AB) as the cathode. S/AB was prepared by milling sulfur with acetylene black in the mass ratio of 2 : 1 then heating at 155 °C for 12 h. The cathode was prepared by mixing S/AB and poly(vinylidene fluoride) binder with a weight ratio of 9 : 1 with N-methyl-2-pyrrolidone as the solvent. The aluminum foil loaded with cathode materials were cut into round disks (1.2 cm in diameter) with an average mass loading of 2.5 mg. The full cells were cycled between 1.5 and 2.8 V at 500 mA g^{-1}.

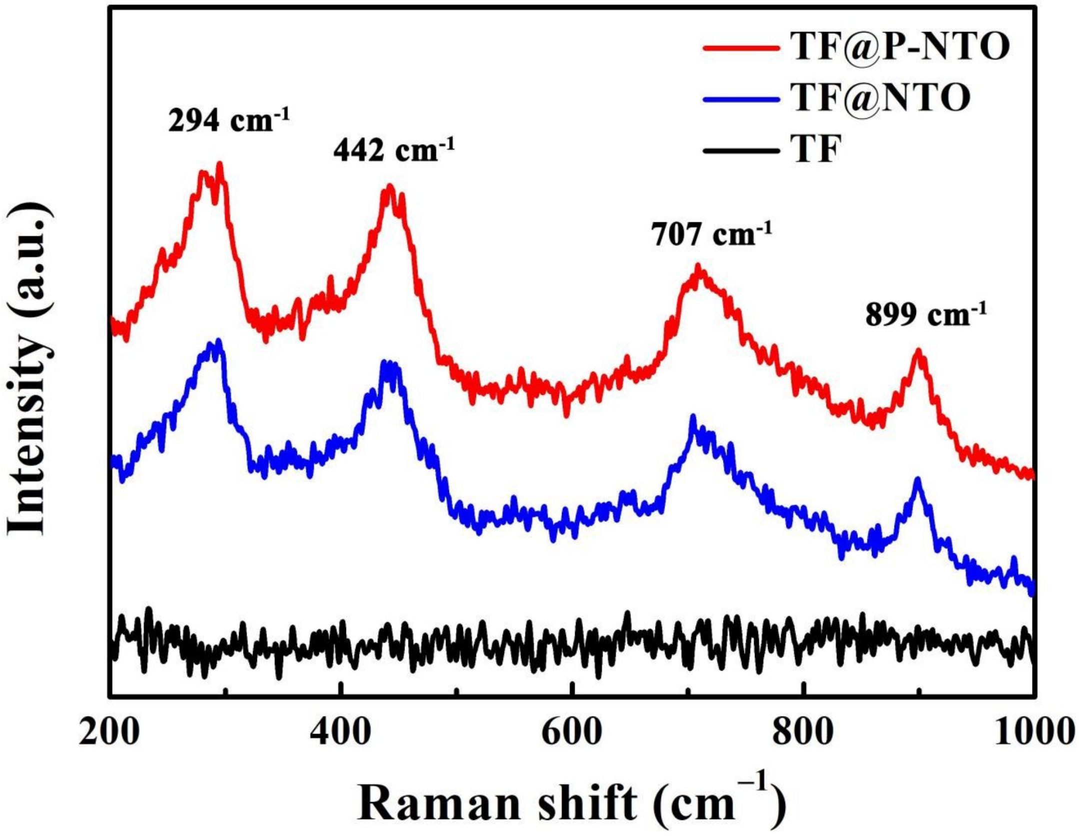

Fig. S1 Raman spectra of TF, TF@NTO and TF@P-NTO.

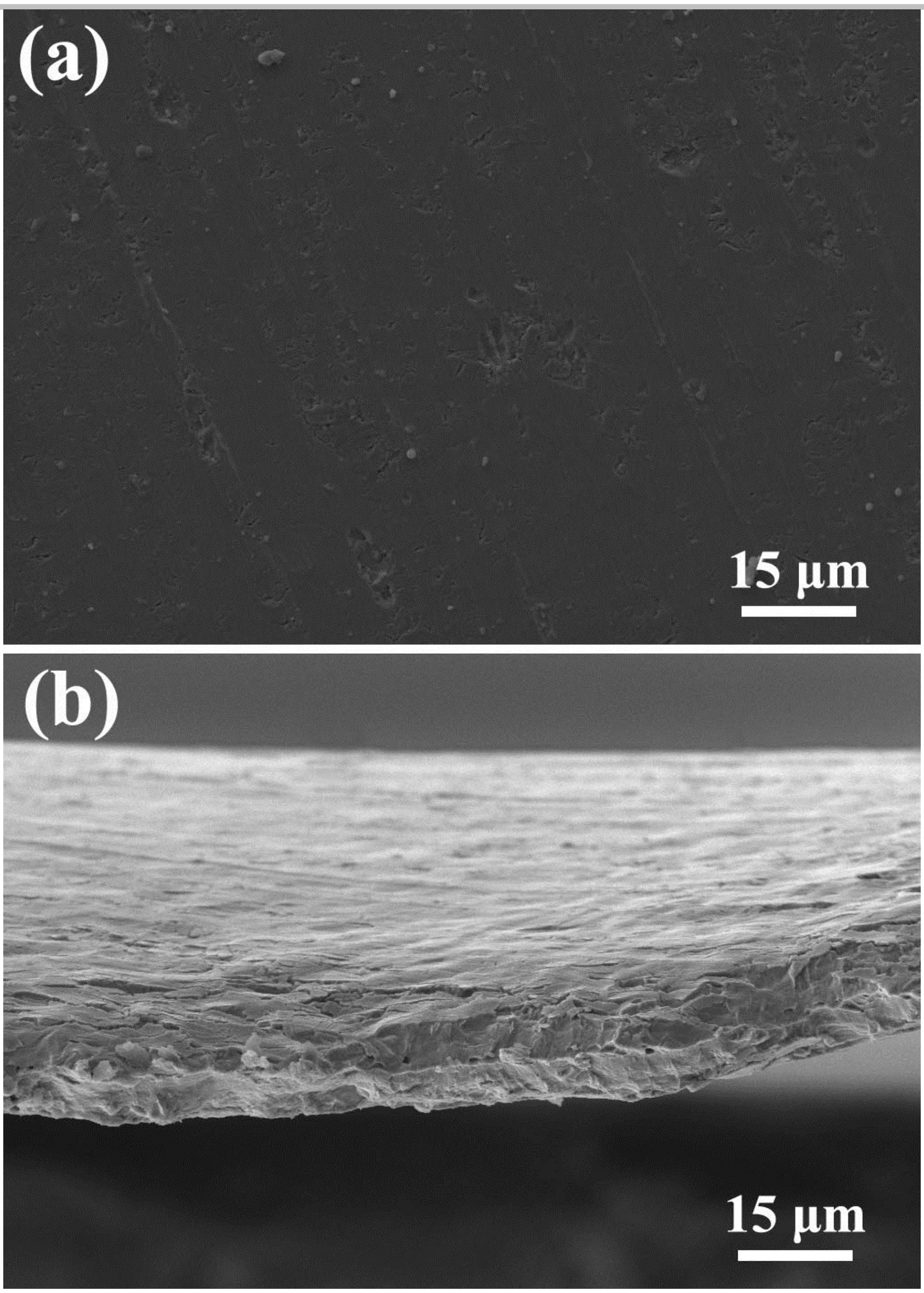

Fig. S2 Top (a) and cross-section (b) SEM images of TF.

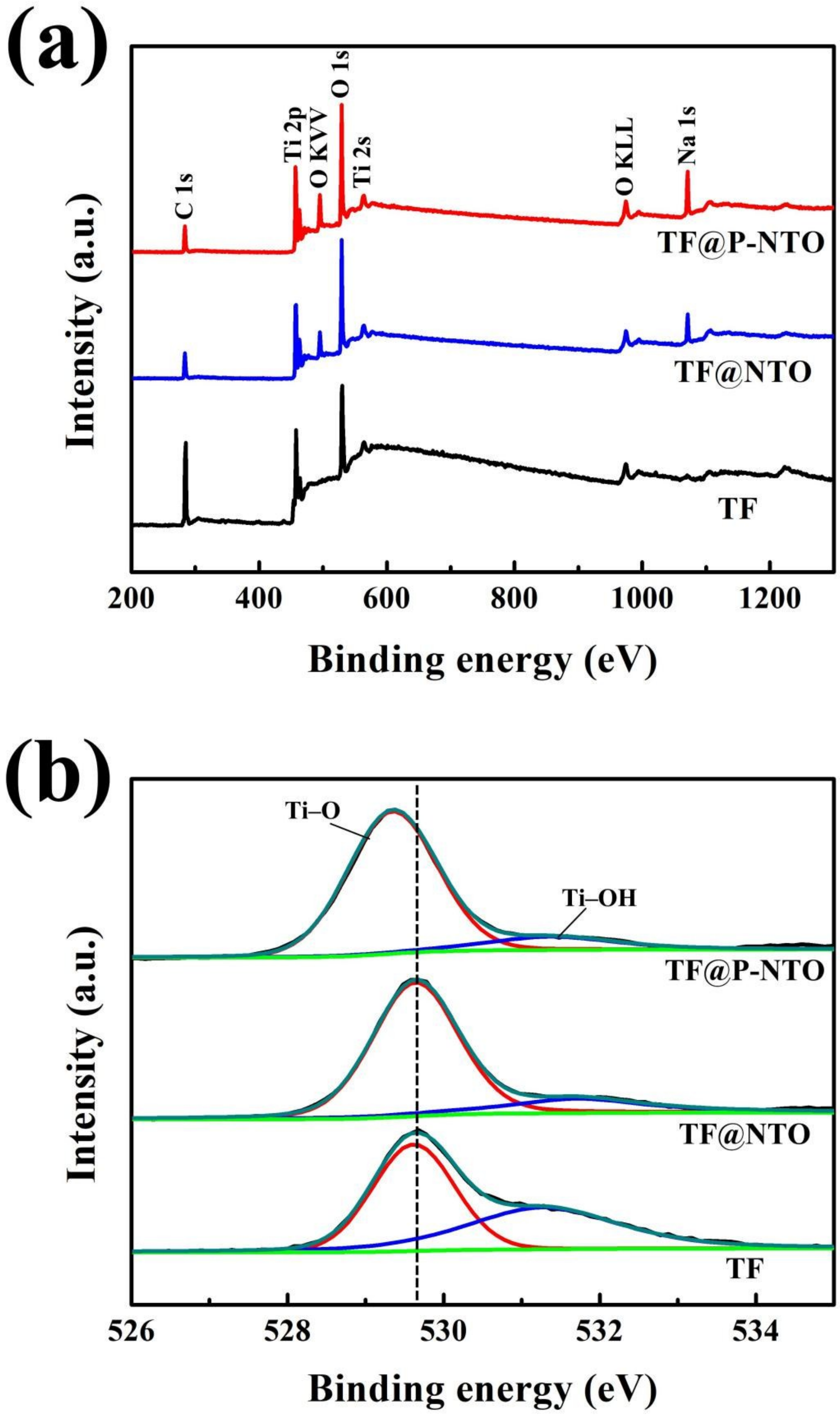

Fig. S3 XPS survey (a) and O 1s XPS spectrum (b) of TF, TF@NTO and TF@P-NTO.

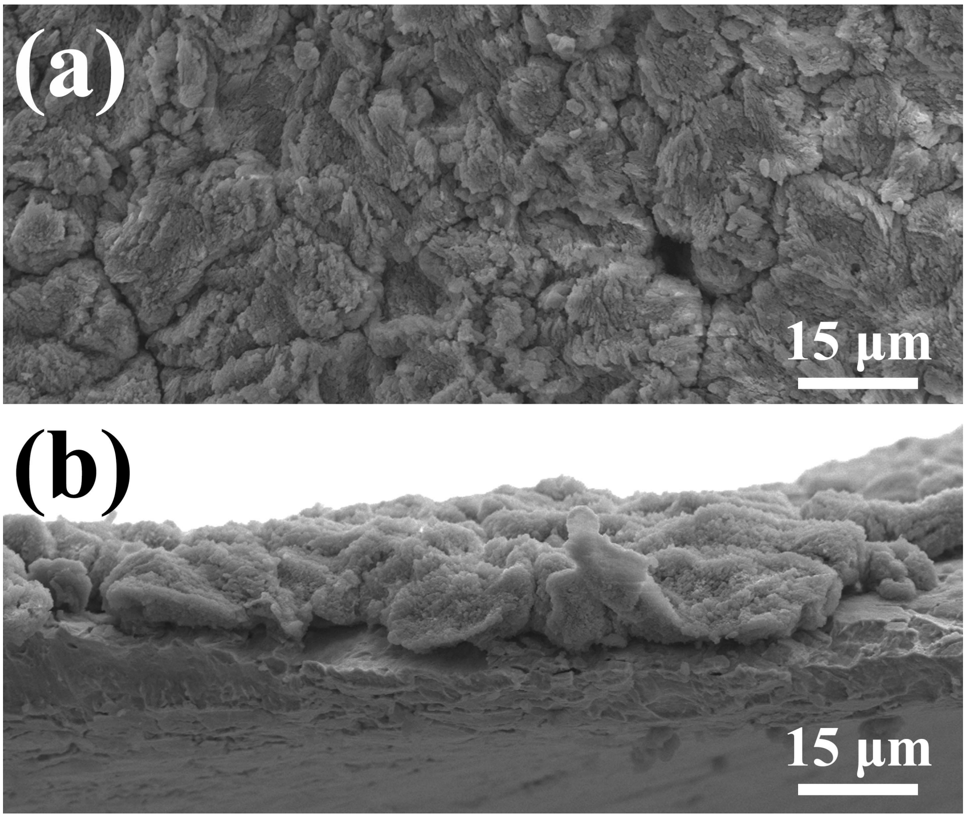

Fig. S4 SEM images of TF after the first lithium plating.

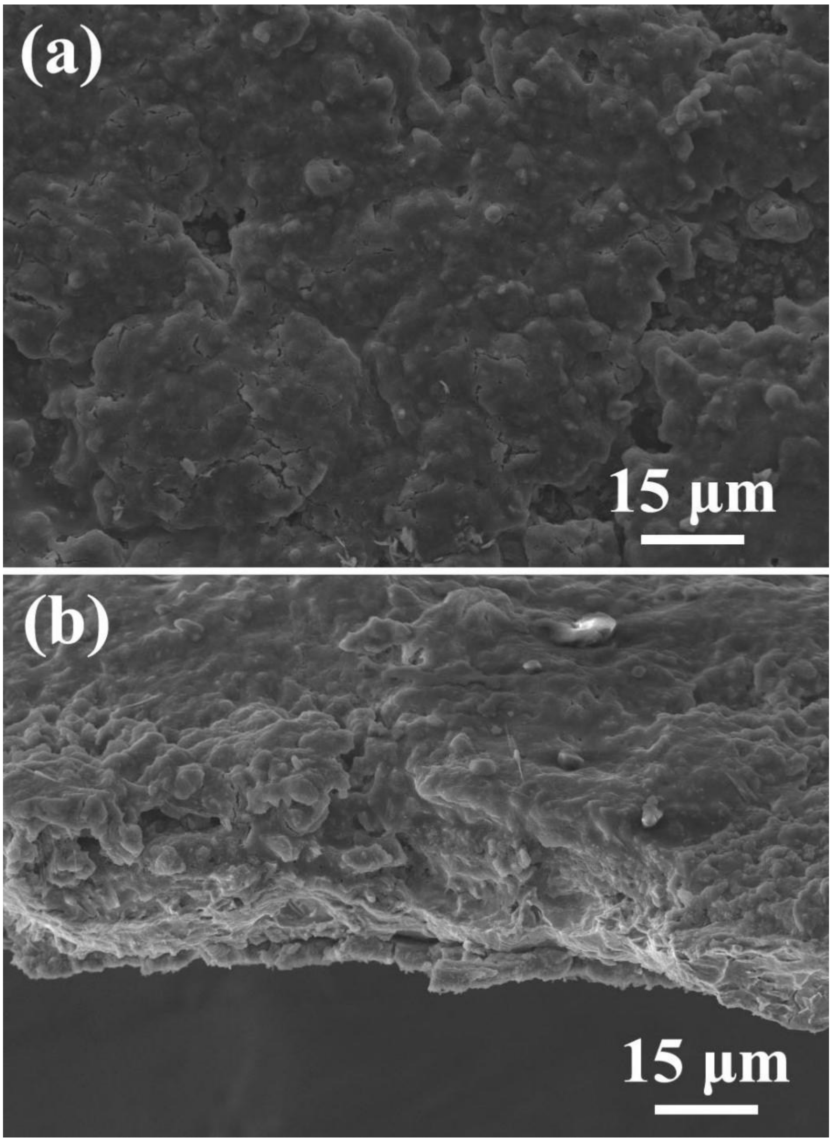

Fig. S5 SEM images of TF@NTO after the first lithium plating.

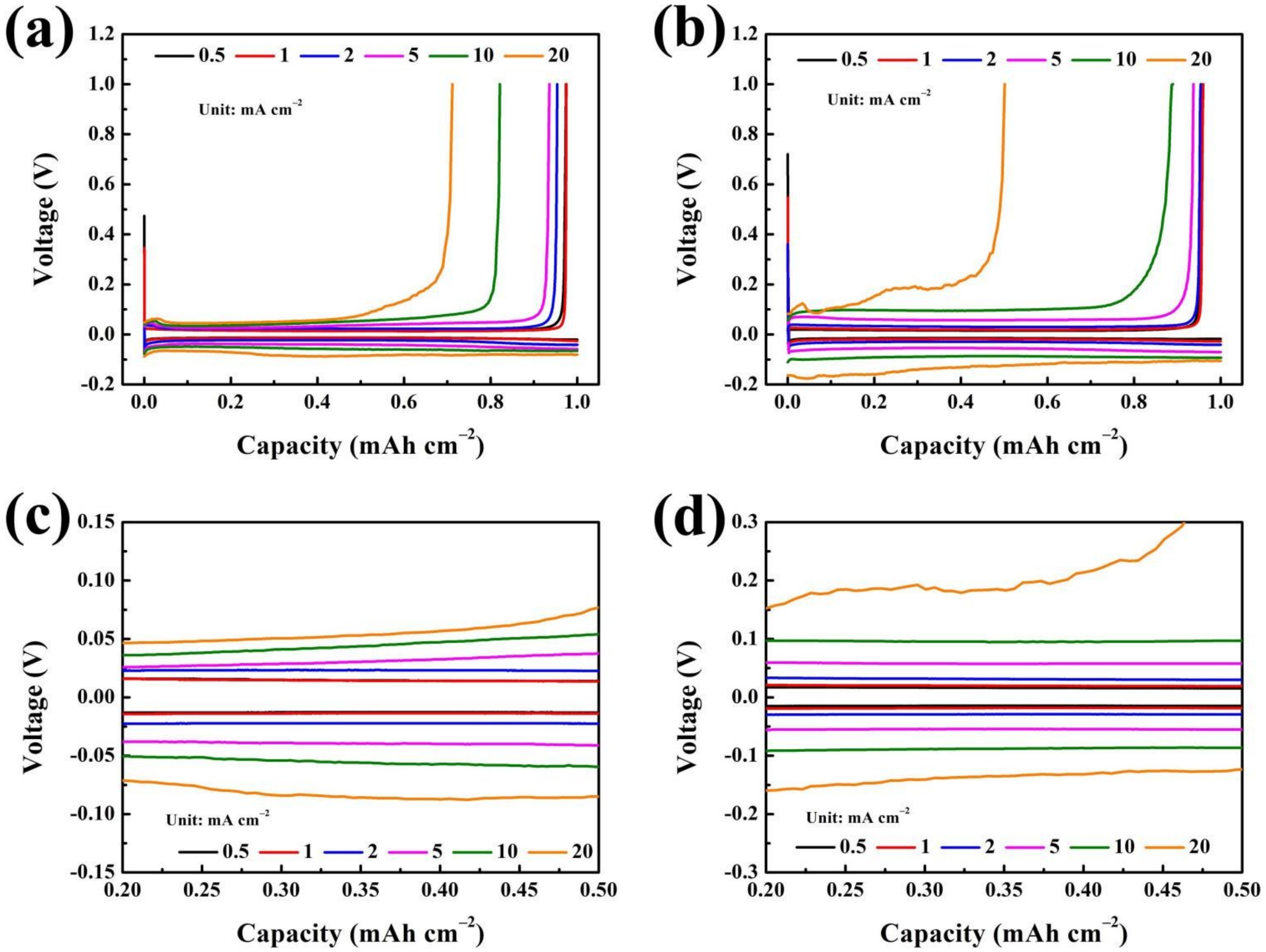

Fig. S6 Plating/stripping profiles of TF (a) and TF@NTO (b) measured at different current densities. The magnified images of TF (c) and TF@NTO (d) from 0.1 to 0.5 mAh cm^{-2}.

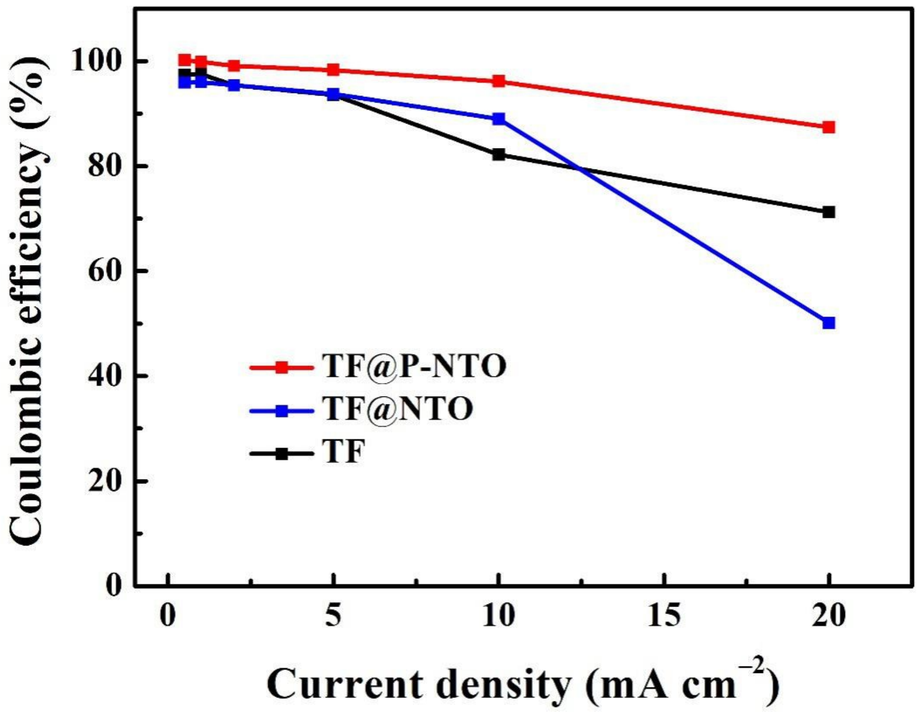

Fig. S7 Rate performance comparison of TF, TF@NTO and TF@P-NTO.

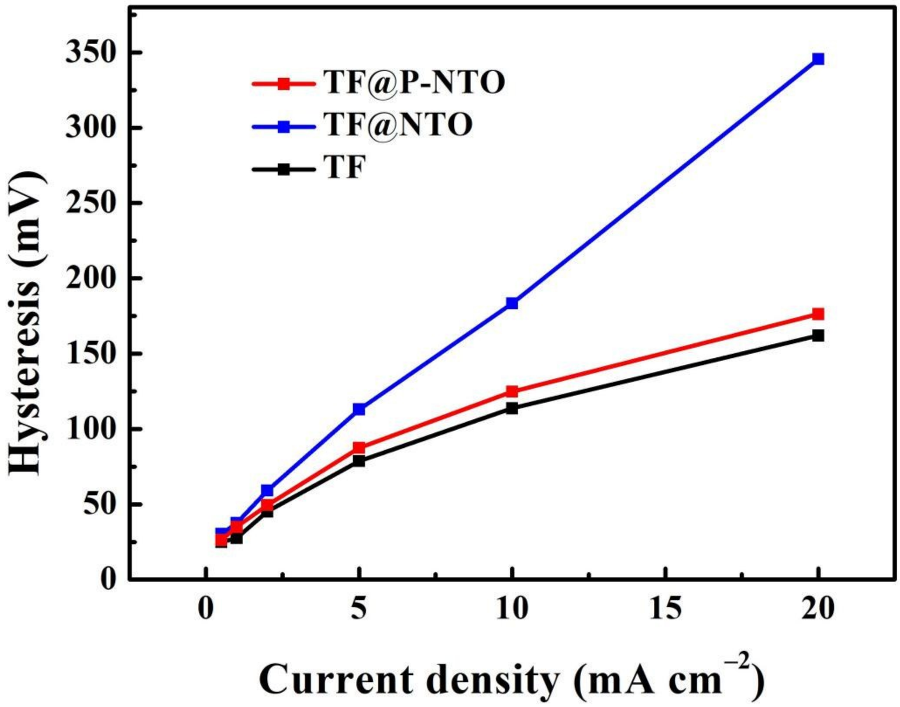

Fig. S8 Voltage hysteresis comparison at different current densities.

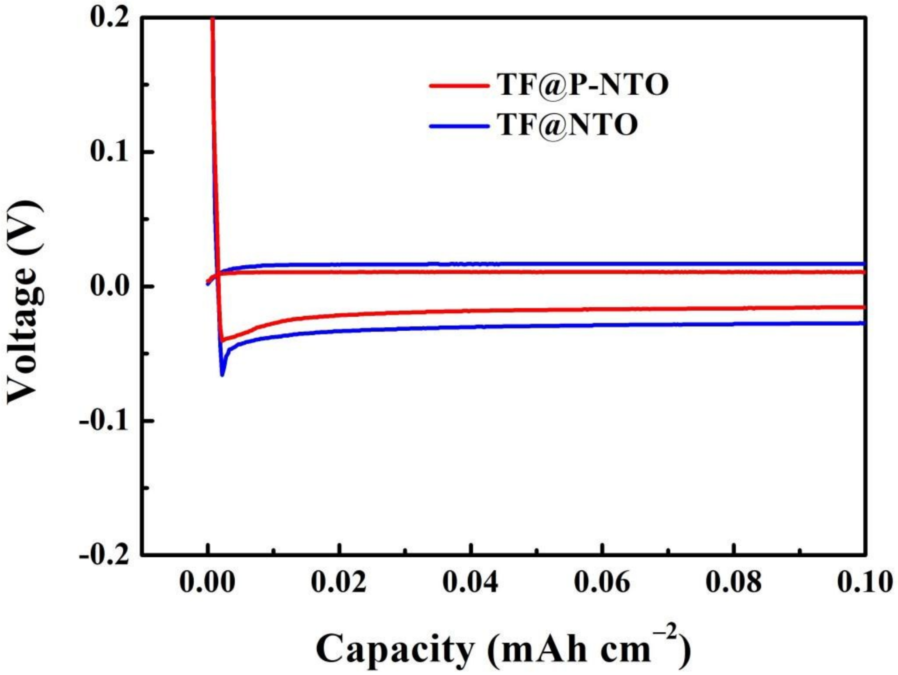

Fig. S9 Magnified image of voltage–capacity curves of TF@NTO and P-TF@NTO at 50th cycle from 0 to 0.1 mAh cm^{-2}.

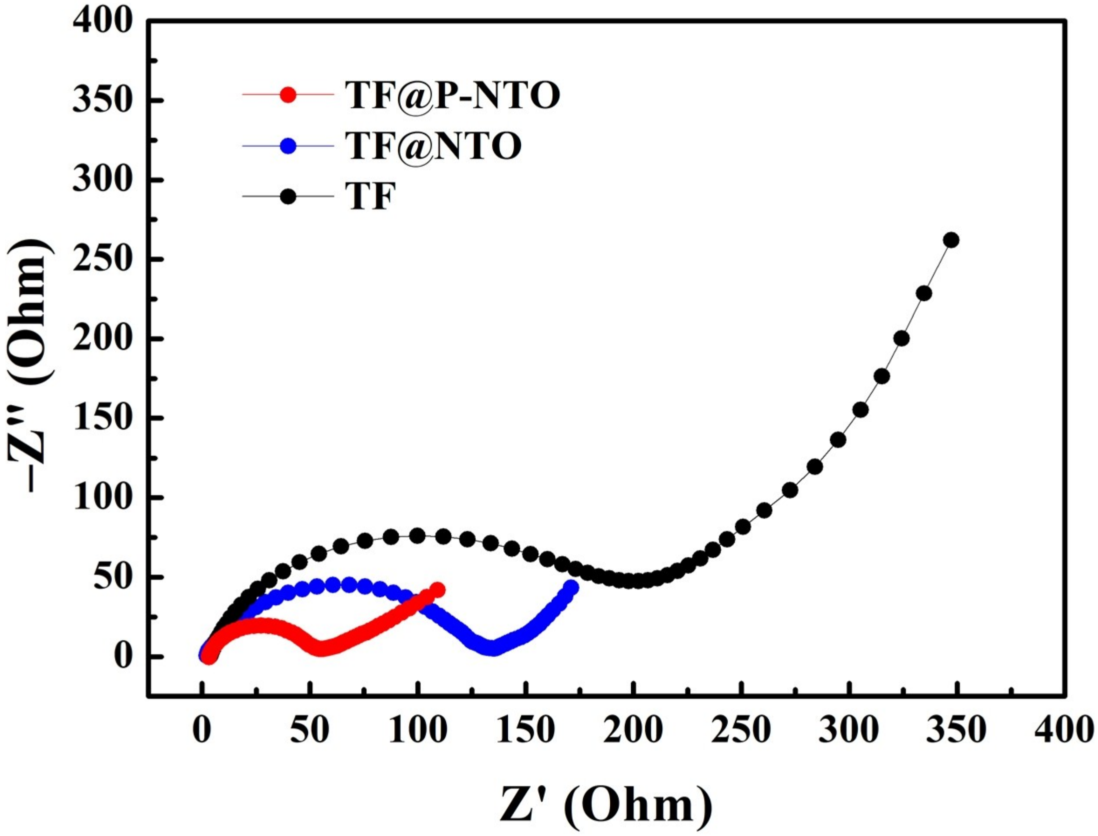

Fig. S10 Electrochemical impedance spectroscopy of P-TF@NTO, TF@NTO and TF after 5 cycles.

Table S1 Comparison of the electrochemical performance of several materials.

Materials	Current density	Cycle number	Coulombic efficiency	Ref.
AlF_3-modified carbon nanofibers	1 mA cm^{-2}	450	97.2%	1
Graphene anchored on Cu foam	2 mA cm^{-2}	150	97.4%	2
Cu-CuO-Ni hybrid structure	1 mA cm^{-2}	250	95%	3
MnO_2 modified Cu foil	0.5 mA cm^{-2}	150	97%	4
3D TiC/C core/shell nanowire skeleton	0.5 mA cm^{-2}	100	98.5%	5
Ti^{3+}-doped Sodium Titanate Nanosheet Arrays on Titanium Foil	1 mA cm^{-2}	150	99.6%	This work

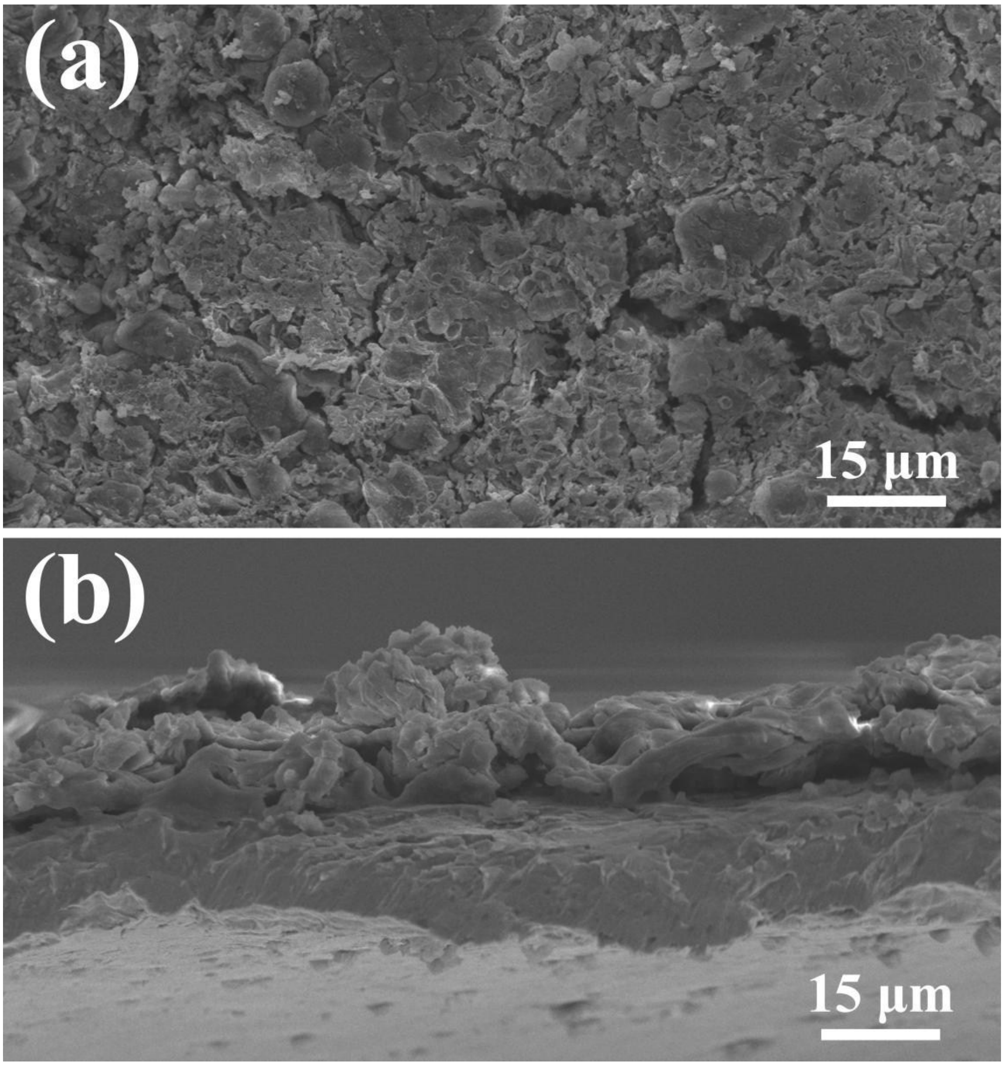

Fig. S11 Top and cross-section SEM images of TF after the 20th lithium plating.

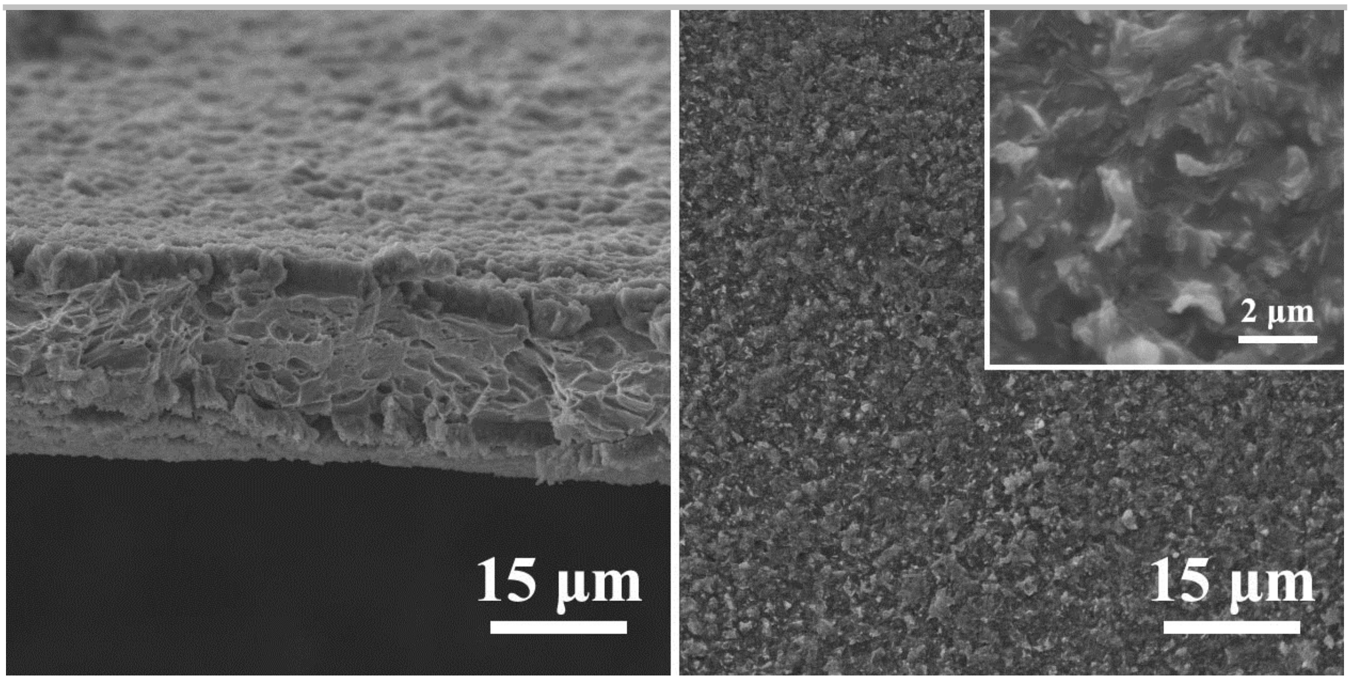

Fig. S12 Top and cross-section SEM images of P-TF@NTO after the 50th lithium stripping.

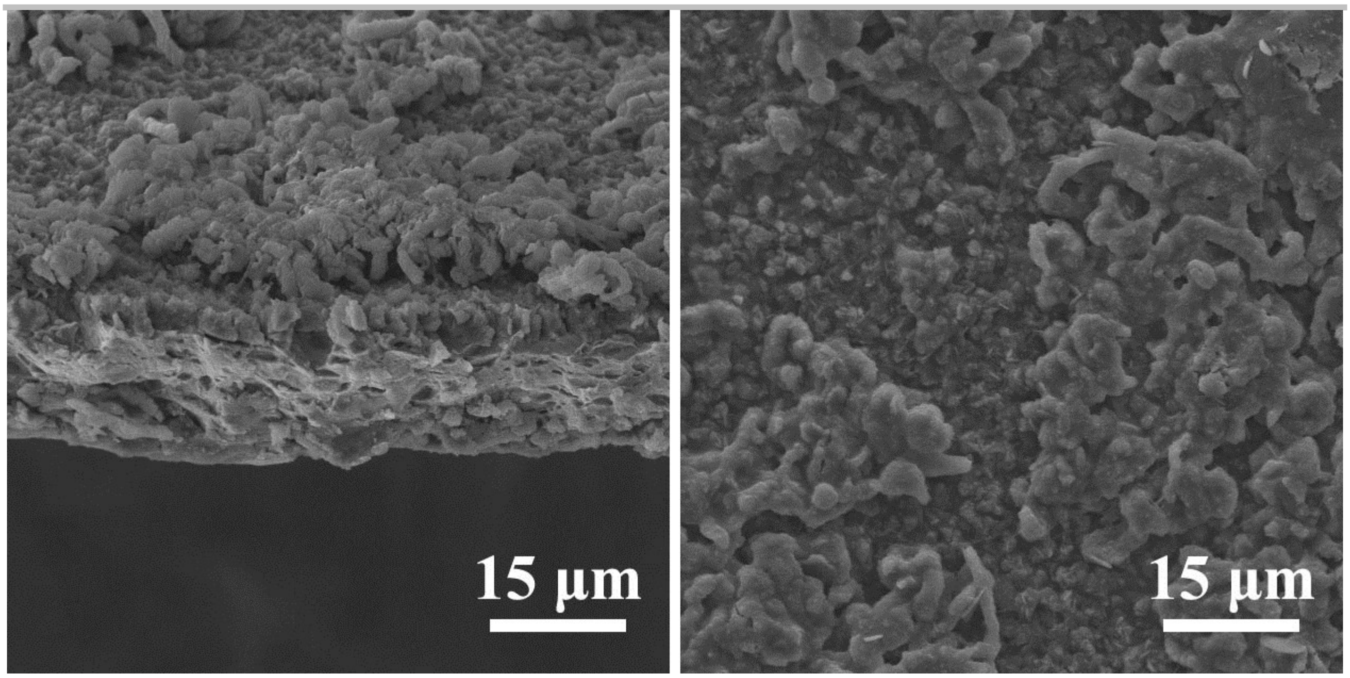

Fig. S13 Top and cross-section SEM images of TF@NTO after the 50th lithium stripping.

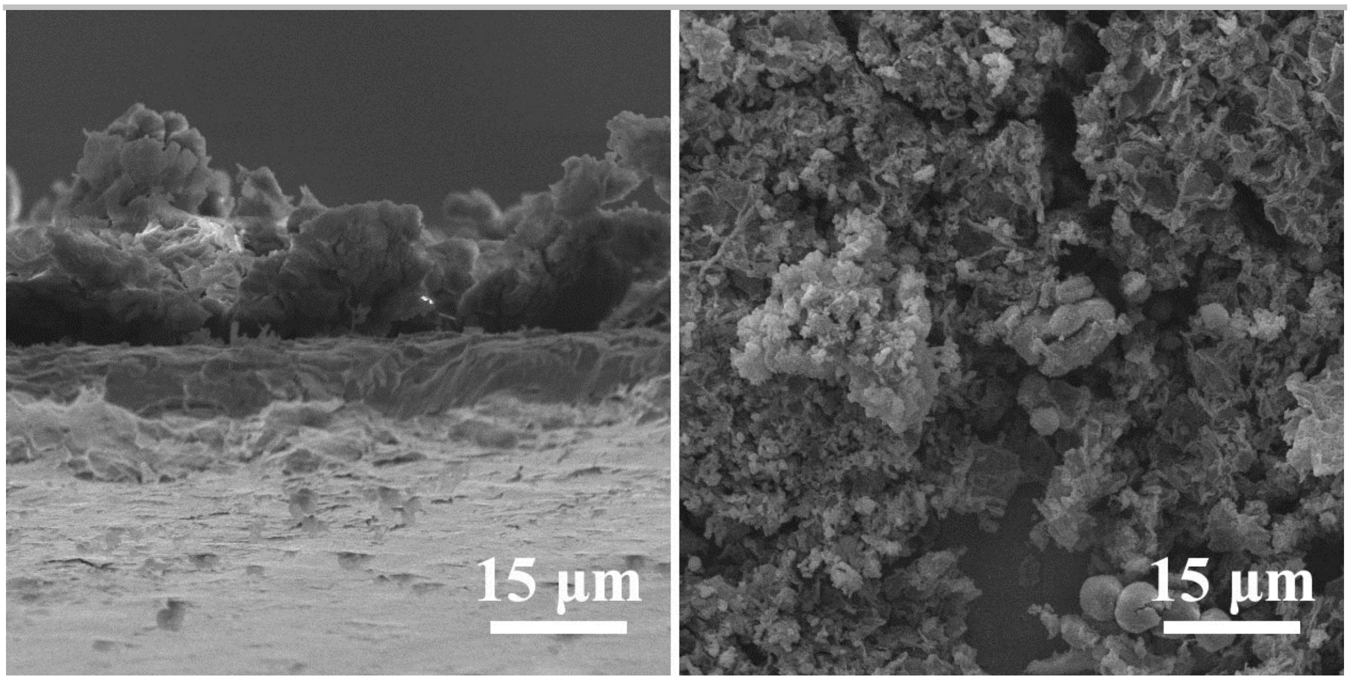

Fig. S14 Top and cross-section SEM images of TF after the 20th lithium stripping.

References

1. C. Guo, H. Yang, A. Naveed, Y. Nuli, J. Yang, Y. Cao, H. Yang and J. Wang, *Chem. Comm.*, 2018, **54**, 8347.
2. G. Yang, J. Chen, P. Xiao, P. O. Agboola, I. Shakir and Y. Xu, *J.Mater. Chem. A*, 2018, **6**, 9899.
3. S. Wu, Z. Zhang, M. Lan, S. Yang, J. Cheng, J. Cai, J. Shen, Y. Zhu, K. Zhang and W. Zhang, *Adv. Mater.*, 2018, **30**, 1705830.
4. M. Hu, Y. Yuan, M. Guo, Y. Pan and D. Long, *J. Mater. Chem. A*, 2018, **6**, 14910-14918.
5. S. Liu, X. Xia, Y. Zhong, S. Deng, Z. Yao, L. Zhang, X.B. Cheng, X. Wang, Q. Zhang and J. Tu, *Adv. Energy Mater.*, 2018, **8**, 1702322.